

Investigation of two- and three-bond carbon–hydrogen coupling constants in cinnamic acid based compounds

Gregory K. Pierens,* Taracad K. Venkatachalam and David C. Reutens

ABSTRACT Two- and three-bond coupling constants ($^2J_{\text{HC}}$ and $^3J_{\text{HC}}$) were determined for a series of 12 substituted cinnamic acids using a selective 2D inphase/antiphase (IPAP)-single quantum multiple bond correlation (HSQMBC) and 1D proton coupled ^{13}C NMR experiments. The coupling constants from two methods were compared and found to give very similar values. The results showed coupling constant values ranging from 1.7 to 9.7 Hz and 1.0 to 9.6 Hz for the IPAP-HSQMBC and the direct ^{13}C NMR experiments, respectively. The experimental values of the coupling constants were compared with discrete density functional theory (DFT) calculated values and were found to be in good agreement for the $^3J_{\text{HC}}$. However, the DFT method underestimated the $^2J_{\text{HC}}$ coupling constants. Knowing the limitations of the measurement and calculation of these multibond coupling constants will add confidence to the assignment of conformation or stereochemical aspects of complex molecules like natural products. Copyright © 2016 John Wiley & Sons, Ltd.

Keywords: NMR; heteronuclear coupling constants; DFT; $^2J_{\text{HC}}$; $^3J_{\text{HC}}$; cinnamic acid; IPAP-HSQMBC

Introduction

Long-range $^nJ_{\text{HH}}$ and $^nJ_{\text{CH}}$ coupling constants have played an important role in the structure elucidation of synthetic compounds and natural products. The measurement of ^1H – ^1H coupling constants is well defined either by direct measurement or simulation of the multiplet of interest, but there is no general method of measuring ^1H – ^{13}C coupling constants. There are two general strategies employed today for measuring the long-range heteronuclear coupling constants. The first is HSQC-TOCSY based pulse sequence strategies.^[1–4] Although these experiments are useful they are unsuitable for coupling constants involving quaternary carbons. The second method either uses long-range optimised HMBC^[5] or HSQMBC^[6] pulse sequences. These methods are highly suited for measuring coupling constants between non-protonated carbons but suffer from the problem of time consuming post processing and antiphase multiplets. Other experiments like EXCID^[7], HSQC-HECADE^[8] and J -HMBC^[9], in which the $^nJ_{\text{CH}}$ coupling evolves in the indirect dimension, have been successfully applied but require long experimental time to achieve the desired resolution. Recently, Parella *et al.*^[10–15] used selective HSQMBC experiments acquired in two different modes, inphase and antiphase (IPAP), to extract the $^nJ_{\text{CH}}$ coupling constants. The processing of the data involves two steps, in which the data are added (IP + AP) and subtracted (IP – AP), and the corresponding rows from these 2D datasets are compared to extract the $^nJ_{\text{CH}}$.

Quantum mechanical calculations of NMR parameters such as chemical shifts and coupling constants have become a very popular tool for synthetic and natural product chemistry for the assignment of stereochemistry within a molecule of interest. Calculation of NMR chemical shifts has been reviewed extensively.^[16–25] These calculations have also been used for the reassignment of structures in complex molecules, such as natural products, in which validation of the proposed structure by gold standard methods like X-ray

crystallography or total synthesis is difficult to achieve. In this regard, it would be very useful to compare the experimental and calculated $^nJ_{\text{CH}}$ coupling constants to validate the structure of the molecule of interest. In a recent report by Kutateladze *et al.*^[26] in 2015 it was shown that using a new basis set (DU8) and the NBO hybridization parameters yielded excellent accuracy of 0.29 Hz (rmsd) for the coupling constant with the maximum unassigned error not exceeding 1 Hz in a diverse collection of natural products. All calculated coupling constants are reported in the Supporting Information (S3–14).

We aim to use 1D (direct) and 2D selective NMR (IPAP-HSQMBC^[10]) experiments to measure the two- and three-carbon–hydrogen coupling constants in 12 cinnamic acid-based compounds, to use the recently described density functional theory (DFT) methods of Kutateladze^[26] to calculate two- and three-carbon–hydrogen coupling constants and to compare the calculated with the experimentally measured coupling constant values. Consistency between measured and calculated heteronuclear long-range coupling constants enhances confidence in the reported structures for compounds.

Experimental

Synthesis

Synthesis of cinnamic acid ester derivatives was carried out using modified literature procedures.^[27–31] In brief, the appropriately substituted cinnamic acid derivative, excess of the alcohol (metha-

* Correspondence to: Gregory K. Pierens, Centre for Advanced Imaging, The University of Queensland, St Lucia, Brisbane 4072, Australia. E-mail: g.pierens@uq.edu.au

Centre for Advanced Imaging, The University of Queensland, Brisbane, Australia

nol, ethanol or isopropanol) and HCl (10 M) were heated at reflux for 8 h. The solvent was evaporated, and the residue was treated with ice cold aqueous sodium hydroxide, and the undissolved material was extracted with ethyl acetate. The organic layer was washed twice with aqueous sodium hydroxide followed by brine and finally dried over anhydrous sodium sulfate. Filtration and evaporation of the solvent gave the desired esters. The esters were either solid and or viscous liquids. The compounds were checked using routine analytical techniques to confirm the structure of the compounds. Each of the samples was subjected to complete NMR structure verification using ^1H , ^{13}C , COSY, HSQC and HMBC.

NMR Spectroscopy

All cinnamic acid derivatives were dissolved in DMSO- d_6 . NMR experiments were recorded on a BRUKER 700 Avance III HD with a three-channel 5-mm TCI cryoprobe incorporating a z-gradient coil. All data were acquired and processed with TOPSPIN v3.2. The NMR samples contained approximately 50–100 mg dissolved in 600 μl DMSO- d_6 .

The ^{13}C NMR data were acquired using the Bruker pulse sequence 'zgpg' experiment with a 60° pulse and with proton decoupling turned off (0 watts). The number of points acquired was 128 k and the sweep width was 80 or 228 ppm.

All ^1H - ^{13}C IP- and AP-HSQMBC experiments were separately recorded.^[10] The recycle delay was set to 1 s, number of scans set to 4 and the interpulse Δ delay ($=1/4^n J_{\text{CH}}$) was set using 8 Hz. The selective 180 pulse was Gaus1_180r.1000 of length 20 ms. The sweep width was 5 ppm centred on the chemical shift of interest. There were 4096 and 128 points acquired in F2 and F1, respectively. Total acquisition time for each experiment was 15 min. IP and AP data were added/subtracted in the time-domain. Prior to Fourier transformation of each data set, zero filling to 8192 points in F2 (digital resolution of 0.43 Hz), 1024 points in F1 and a sine squared function in both dimensions were applied. The corresponding rows from the addition and subtraction dataset were compared, and the coupling constant was extracted from the multiplet offset.

Computational Calculation (DFT)

Monte Carlo Conformational searching was performed using Macromodel (Schrodinger Inc)^[32] for all compounds. Torsional sampling (MCM) was performed with 1000 steps per rotatable bond. Each step was minimised with the OPLS-2005 force field using the Truncated Newton Conjugate Gradient (TNCG) method with maximum iterations set at 50 000 and energy convergence threshold at 0.02. All other parameters were default values. The resulting number of unique conformations are shown in Table 1. All

conformations were further optimised, and Natural Bond Orbital (NBO), chemical shift and coupling constants calculated in Gaussian^[33] (see Supporting Information for an example of the Gaussian script for acetic acid (S2)).

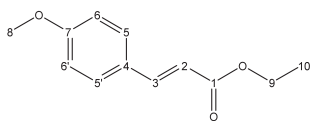
The $^n J_{\text{HC}}$ coupling constants were calculated using the method of Kutateladze and Mukhina.^[34] The data were pre-processed using the Python script supplied from Kutateladze web site, and the resulting file was up loaded to Kutateladze web site for processing (<http://kgroup.du.edu/nmr>).

Results and Discussion

In the present study a set of 12 compounds consisting of substituted cinnamic acids and ester derivatives was synthesised using a modification of a previously described procedure (see Experimental section). The cinnamic acid skeleton was functionalized at two sites. The aromatic moiety in the structure was functionalized in the *para*-position with electron donating and withdrawing groups. This was done to examine the effect of functional groups electronic influence on the coupling constants associated with protons and carbons in the structure. Additionally, the carboxylic acid moiety was esterified with three different alkyl groups. The three different group were used to evaluate any steric bulk influence on the magnitude of experimentally determined coupling constants. Table 1 shows the structure of the 12 derivatives prepared in the present study.

Initially, the $^1 J$ coupling constants were measured directly on a subset of compounds (**3**, **6**, **8** and **11**) via a ^1H coupled ^{13}C NMR

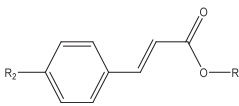
Table 2. $^1 J_{\text{CH}}$ coupling constants for compounds **3**, **6**, **8** and **11** and the numbering scheme used



| Position | Compounds, $^1 J_{\text{CH}}$ | | | |
|----------|-------------------------------|----------|----------|-----------|
| | 3 | 6 | 8 | 11 |
| 2 | 162.6 | 164.4 | 162.1 | 161.9 |
| 3 | 159.2 | 159.5 | 154.9 | 154.9 |
| 5,5' | 165.5 | 165.8 | 159.5 | 159.5 |
| 6,6' | 169.6 | 169.4 | 160.9 | 160.6 |
| 8 | — | — | 144.3 | 144.9 |
| 9 | — | 147.4 | 147.4 | 148.1 |
| 10 | — | — | 126.7 | 126.4 |

—: not in compound.

Table 1. The structural features of 12 cinnamic acid derivatives used in the present study and the number of conformers used in the DFT calculations



| Compound | 1 | 2 | 3 | 4 | 5 | 6 | 7 | 8 | 9 | 10 | 11 | 12 |
|-----------------|----------|----------|-----------------|----------|----------|-----------------|----------|----------|-----------------|--------------|--------------|-----------------|
| R ₁ | H | H | H | Me | Me | Me | Et | Et | Et | <i>i</i> -Pr | <i>i</i> -Pr | <i>i</i> -Pr |
| R ₂ | H | OMe | NO ₂ | H | OMe | NO ₂ | H | OMe | NO ₂ | H | OMe | NO ₂ |
| # of conformers | 2 | 4 | 2 | 2 | 4 | 2 | 4 | 8 | 4 | 2 | 4 | 2 |

experiment, and the results are shown in Table 2. The numbering of the protons/carbons associated with the structure are also shown in Table 2. On examination of the coupling constants, it was observed that the 1J coupling constants were consistent for C3 in the compounds with the same aromatic moieties, i.e. the nitro compounds (**3** and **6**) having a larger coupling of ~ 159 Hz compared to the methoxy compound (**8** and **11**) of ~ 155 Hz. From these results, it was evident that the functionalisation of the acid moiety with different ester groups does not significantly change the coupling constant for C3. This trend is also seen for C5/5' and C6/6', with the nitro substituted compounds (**3** and **6**) having a 6 and 8-Hz change from the methoxy compounds (**8** and **11**), respectively. Based on the results we may conclude that the nature of the substitution at the 4-position of the phenyl ring does affect the magnitude of observed coupling constant values. For C2, it appears that the free acid, ethyl and isopropyl esters seem to give the same 1J coupling constant of 161.9–162.6 Hz, but the methyl ester approximately 2 Hz higher coupling constant of 164.4 Hz.

Interestingly, on further examination of these spectra, the majority of the carbon resonances were more complex than first expected. Direct extraction of $^2J_{\text{CH}}$ and $^3J_{\text{CH}}$ coupling constants was possible. Proton-coupled carbon NMR experiments were used regularly in the early years of NMR to assign the number of protons directly attached to carbon atoms i.e. C (s), CH (d), CH₂ (t) and CH₃ (q), whereas DEPT^[35] or edited HSQC is now used almost exclusively. An example of these couplings can be seen in Fig. 1 in which the carbonyl carbon (C1) shows the expected increase in complexity as the number of coupling partners increases. This data can be used to extract the $^2J_{\text{CH}}$ and $^3J_{\text{CH}}$ coupling constants when large amounts of material are available because of the low sensitivity of acquiring ^{13}C NMR.

The four compounds (**3**, **6**, **8** and **11**) were used as a test subset to extract the long-range coupling constants from the proton-coupled ^{13}C spectrum. Many of the first-order multiplets were used; however, C6/6' were not used to extract any coupling information because of the second-order appearance of the multiplet. Interestingly, the C5/5' multiplet could be used for extracting coupling constants. The DAISY programme (V3, 2014) within Topspin (V3.5 pl2) was used to extract the couplings and chemical shifts by simulation.

The coupling constants are shown in Table 3. As can be seen there is very little difference between the corresponding coupling constants for the similar $^2J_{\text{HC}}$ or $^3J_{\text{HC}}$ in these compounds. One of the largest differences is for the $^3J_{\text{HC1}}$ in the methyl, ethyl and isopropyl esters, where the methyl ester had the largest coupling of 3.88 Hz and the isopropyl ester had the smallest coupling with 2.97 Hz. The $^2J_{\text{H6/6'}}$ also showed a significant difference. This is understandable because this carbon has either a nitro (**3** and **6**) or methoxy (**8** and **11**) group attached at the 4-position of the aromatic ring which seems to result in a ~ 0.8 -Hz reduction in coupling constant going from a nitro to methoxy moiety. This result is

Table 3. Subset of $^2J_{\text{CH}}$ and $^3J_{\text{CH}}$ coupling constants measured from the proton-coupled carbon spectra for compounds **3**, **6**, **8** and **11**

| $^nJ_{\text{HC}}$ | Compounds | | | |
|-------------------|------------|------------|------------|------------|
| | 3 | 6 | 8 | 11 |
| H2–C1 | 2.55 | 2.38 | 2.47 | 2.40 |
| H2–C3 | 1.34 | 1.56 | 1.09 | 1.11 |
| H2–C4 | 5.41 | 5.48 | 5.58 | 5.58 |
| H3–C1 | 6.78 | 6.91 | 6.84 | 6.82 |
| H3–C2 | 3.11 | 3.27 | 3.00 | 3.12 |
| H3–C4 | 2.08 | 2.01 | 2.22 | 2.33 |
| H3–C5 | 5.09 | 5.03 | 5.00 | 5.26 |
| H5/5'–C3 | 4.44 | 4.48 | 4.49 | 4.50 |
| H5/5'–C4 | ≤ 0.7 | ≤ 0.7 | ≤ 0.7 | ≤ 0.7 |
| H5/5'–C7 | 9.59 | 9.61 | 9.26 | 9.32 |
| H5–C5' | 6.92 | 7.01 | 7.39 | 7.37 |
| H6/6'–C4 | 7.78 | 7.77 | 7.26 | 7.29 |
| H6/6'–C7 | 3.42 | 3.43 | 2.61 | 2.78 |
| H6–C5 | ≤ 0.7 | ≤ 0.7 | ≤ 0.7 | ≤ 0.7 |
| H8–C7 | NA | NA | 4.16 | 4.23 |
| H9–C1 | NA | 3.88 | 3.13 | 2.97 |
| H9–C10 | NA | NA | 2.63 | 1.61 |
| H10–C9 | NA | NA | 4.42 | 4.24 |
| H10'–C10 | NA | NA | NA | 4.71 |

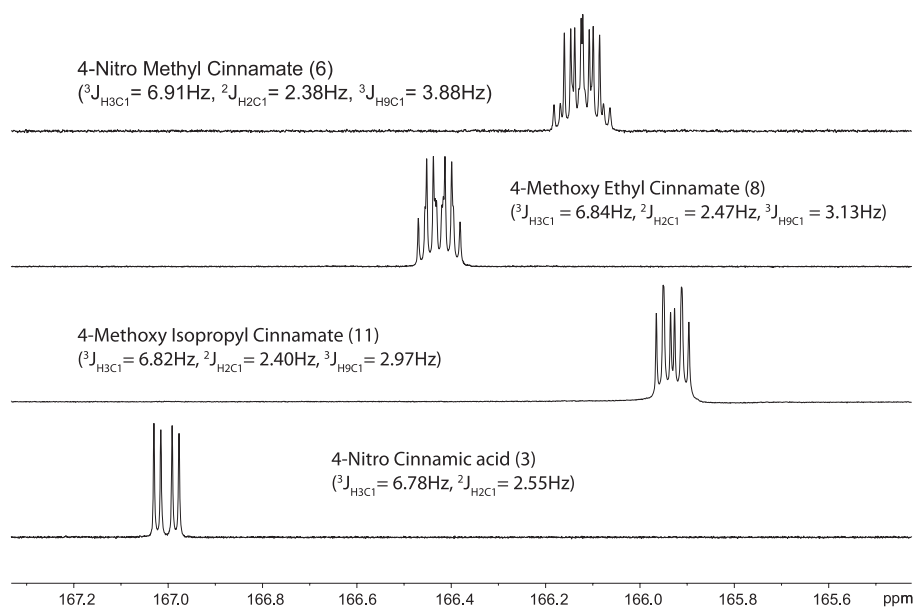


Figure 1. The carbonyl carbon (C1) from a proton coupled NMR experiment for four different compounds resulting in different multiplicity (**3**, **6**, **8** and **11**).

consistent with the data observed for 1J coupling constants (discussed earlier). There is also a difference in the magnitude of the coupling constant observed between $^2J_{H9C10}$ in the ethyl and isopropyl esters. The ethyl had a value of 2.63 Hz while this decreased to 1.61 Hz for the isopropyl ester. Therefore, we can see there is a small difference because of the change in structure. From now on, we will use the coupling constants listed in Table 3 as the 'gold standard' or absolutely correct values for the following comparisons and discussions.

One carbon the authors would like to highlight is C7, which is the most complex of the multiplets examined (Fig. 2). In compounds **8** and **11** having the methoxy group at the *para*-position of the aromatic ring, C7 appears as a very complex multiplet despite having only three coupling partners. In compounds **8** and **11** this carbon is coupled to H5/5', 6/6' and the three methoxy protons (H8) which results in the multiplicity of triplet of triplets of quartets (36 lines). By comparison C7 in the nitro compounds (**3** and **6**) is a triplet of triplets (9 lines). Figure 2 illustrates, both the experimentally and the simulated multiplets obtained for C7 in compound **8**.

The IPAP-HSQMBC sequence was used to measure the $^nJ_{HC}$ coupling constants in all 12 compounds used in this study. This pulse sequence relies on selective excitation of a multiplet. Many of the proton multiplets were used but, when overlapping signals occurred in the spectrum, the measurement became very complicated and sometimes impossible to interpret. The chemical shifts that were measured without ambiguity are shown in Tables 4 and 5 for the $^3J_{HC}$ and $^2J_{HC}$ coupling constants, respectively. Because the $^2J_{HC}$ and $^3J_{HC}$ coupling constants have been measured using two different experiments for the subset of four compounds (**3**, **6**, **8** and **11**), the coupling constants from the ^{13}C and IPAP-HSQMBC methods were plotted against each other for the $^2J_{HC}$ and $^3J_{HC}$ and the graphs are shown in Fig. 3. The $^3J_{HC}$ showed that the two methods are in very good agreement with an average deviation of 0.1 Hz and the largest deviation between H2-C4 of 0.4 Hz for compounds **8** and **11**. Even for the smaller $^2J_{HC}$ coupling constants, both methods also showed a good agreement, but a slightly lower correlation was observed. The average deviation of 0.23 Hz with the largest of

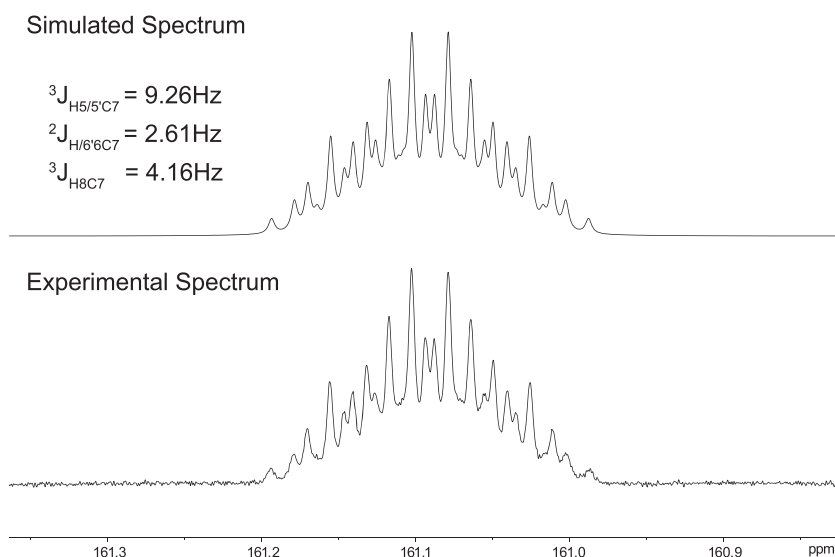


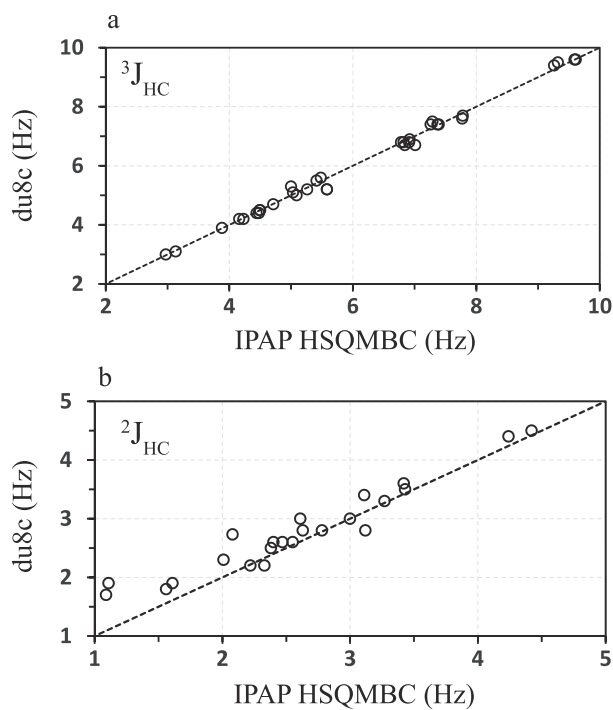
Figure 2. The experimental (proton coupled carbon spectrum) and simulated C7 multiplet of compound **8**.

Table 4. Experimental 3J coupling constants measured by the IPAP-HSQMBC experiment and calculated by method of Kutateladze and Mukhina ("du8c" in parenthesis) for compounds **1–12**

| Compounds | H2-C4 | H3-C1 | H3-C5/5' | H5/5'-C3 | H5/5'-C5'/5 | H5/5'-C7 | H6/6'-C4 | H6/6'-C6'/6 | H8-C7 | H9-C1 | H10-C10 |
|-----------|-----------|-----------|-----------|-----------|-------------|-----------|-----------|-------------|-----------|-----------|-----------|
| 1 | 5.3 (5.3) | 6.8 (7.1) | 5.1 (5.6) | 4.6 (5.1) | 6.4 (6.5) | 7.4 (7.5) | NA (7.5) | NA (7.6) | — | — | — |
| 2 | 5.2 (5.2) | 6.8 (7.0) | 5.4 (5.7) | 4.4 (4.7) | 7.4 (7.3) | 9.4 (9.3) | 7.5 (7.3) | 4.8 (4.6) | 4.1 (4.1) | — | — |
| 3 | 5.5 (5.6) | 6.8 (7.2) | 5.0 (5.7) | 4.4 (4.9) | 6.9 (7.1) | 9.6 (9.5) | 7.7 (7.9) | 4.5 (4.6) | — | — | — |
| 4 | 5.3 (5.3) | 6.9 (7.0) | 5.2 (5.6) | NA (5) | NA (6.5) | NA (7.5) | NA (7.4) | NA (7.6) | — | 4.0 (4.1) | — |
| 5 | 5.3 (5.3) | 6.9 (6.9) | 5.2 (5.7) | 4.6 (4.7) | 7.4 (7.3) | 9.5 (9.3) | 7.5 (7.3) | 4.9 (4.6) | 4.2 (4.0) | 4.0 (4.1) | — |
| 6 | 5.6 (5.6) | 6.8 (7.1) | 5.1 (5.6) | 4.4 (4.9) | 6.7 (7.1) | 9.6 (9.5) | 7.6 (7.9) | 4.7 (4.6) | — | 3.9 (4.2) | — |
| 7 | 5.3 (5.3) | 6.8 (6.9) | 5.1 (5.6) | 4.8 (5.0) | 6.2 (6.5) | 7.5 (7.5) | NA (7.4) | NA (7.5) | — | 3.1 (3.0) | — |
| 8 | 5.2 (5.3) | 6.7 (6.8) | 5.3 (5.7) | 4.5 (4.7) | 7.4 (7.3) | 9.4 (9.3) | 7.5 (7.3) | 5.0 (4.7) | 4.3 (4.0) | 3.1 (3.1) | — |
| 9 | 5.6 (5.6) | 6.8 (7.0) | 5.0 (5.6) | 4.3 (4.8) | 6.8 (7.1) | 9.7 (9.5) | 7.6 (7.9) | 4.6 (4.6) | — | 3.1 (3.1) | — |
| 10 | 5.2 (5.3) | 6.7 (6.9) | 5.1 (5.7) | 4.9 (5) | 6.2 (6.6) | 7.4 (7.5) | NA (7.4) | NA (7.6) | — | 2.9 (3.1) | 4.7 (4.4) |
| 11 | 5.2 (5.3) | 6.8 (6.8) | 5.2 (5.7) | 4.5 (4.7) | 7.4 (7.3) | 9.5 (9.3) | 7.5 (7.3) | 5.0 (4.7) | 4.2 (4.0) | 3.0 (3.2) | 4.6 (4.4) |
| 12 | 5.5 (5.6) | 6.8 (7.0) | 5.1 (5.7) | 4.3 (4.8) | 6.8 (7.1) | 9.7 (9.5) | 7.8 (7.9) | 4.7 (4.6) | — | 2.8 (3.1) | 4.7 (4.3) |

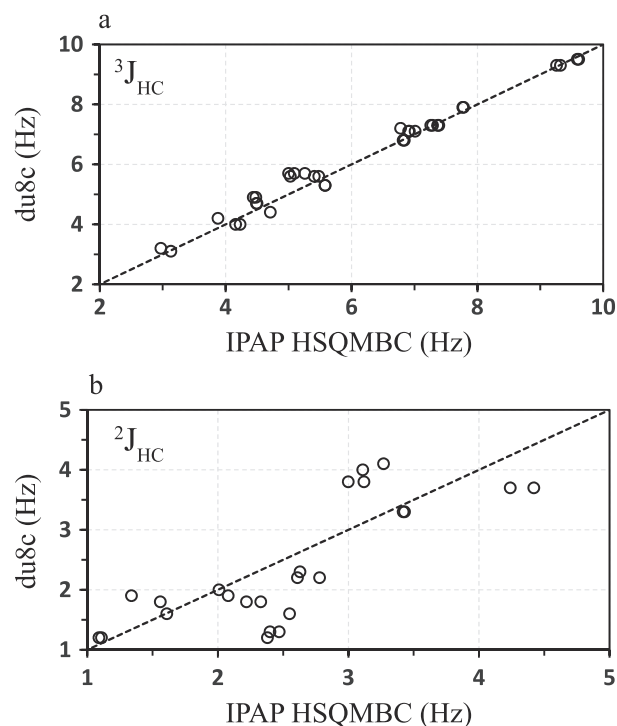
Table 5. 2J coupling constants measured by the IPAP-HSQMBC experiment and calculated by method of Kutateladze and Mukhina (in parenthesis) for compounds 1–12

| Compounds | H2–C1 | H2–C3 | H3–C2 | H3–C4 | H6/6'–C7 | H9–C10 | H10–C9 |
|-----------|-----------|-----------|-----------|-----------|-----------|-----------|-----------|
| 1 | 2.8 (1.8) | 1.8 (1.6) | 3.0 (3.7) | 2.4 (1.7) | NA (1.3) | — | — |
| 2 | 2.7 (1.8) | 1.7 (1.3) | 3.0 (3.7) | 2.4 (1.7) | 2.6 (2.2) | — | — |
| 3 | 2.6 (1.6) | NA (1.9) | 3.4 (4.0) | 2.6 (1.9) | 3.6 (3.3) | — | — |
| 4 | 2.6 (1.4) | 1.8 (1.5) | 3.1 (3.9) | 2.4 (1.8) | NA (1.3) | — | — |
| 5 | 2.6 (1.3) | 1.8 (1.3) | 3.2 (3.8) | 2.3 (1.8) | 2.8 (2.2) | — | — |
| 6 | 2.5 (1.2) | 1.8 (1.8) | 3.3 (4.1) | 2.3 (2.0) | 3.5 (3.3) | — | — |
| 7 | 2.6 (1.4) | 2.0 (1.5) | 3.1 (3.9) | 2.3 (1.8) | NA (1.3) | 2.7 (2.3) | 4.5 (3.7) |
| 8 | 2.6 (1.3) | 1.7 (1.2) | 3.0 (3.8) | 2.3 (1.8) | 3 (2.2) | 2.8 (2.3) | 4.5 (3.7) |
| 9 | 2.4 (1.2) | NA (1.7) | 3.3 (4.1) | 2.4 (2.1) | 3.4 (3.3) | 2.7 (2.4) | 4.5 (3.7) |
| 10 | 2.6 (1.4) | 1.9 (1.4) | 3.2 (3.9) | 2.2 (1.9) | NA (1.3) | 1.9 (1.6) | 4.3 (3.7) |
| 11 | 2.6 (1.3) | 1.9 (1.2) | 3.2 (3.8) | 2.2 (1.8) | 2.8 (2.2) | 1.9 (1.6) | 4.4 (3.7) |
| 12 | 2.4 (1.2) | NA (1.7) | 3.3 (4.1) | 2.4 (2.1) | 3.3 (3.3) | 2.1 (1.6) | 4.3 (3.7) |

**Figure 3.** Comparison of the measured $^3J_{\text{HC}}$ (a) and $^2J_{\text{HC}}$ (b) coupling constants from the direct ^{13}C and the IPAP-HSQMBC experiments for compounds 3, 6, 8 and 11. ($^3J_{\text{HC}}$ (36 coupling constants) and $^2J_{\text{HC}}$ (23 coupling constants)) The dotted line represents a 1:1 correspondence.

H2–C3 of 0.79 Hz for compound **11**. However we found the IPAP-HSQMBC overestimated the $^2J_{\text{HC}}$ coupling values. This could be because of two factors. First, digital resolution, which is lower in the IPAP-HSQMBC experiment (~ 0.8 Hz) compared to the direct carbon (~ 0.3 Hz), and second, during the processing of the IPAP-HSQMBC experiment the datasets are added and subtracted. This could lead to non-complete removal of the proton-proton couplings.

The $^nJ_{\text{HC}}$ coupling constants were calculated using the method of Kutateladze and Mukhina.^[34] From now on we will refer to this method as 'du8c'. The coupling constants (Tables 4 and 5) were compared to the direct ^{13}C method, and the results are shown in Figs 4 and 5. The $^3J_{\text{HC}}$ data showed that there was a very good

**Figure 4.** Comparison of the measured and calculated $^3J_{\text{HC}}$ (a) and $^2J_{\text{HC}}$ (b) from the direct ^{13}C and the du8c method for compounds 3, 6, 8 and 11. ($^3J_{\text{HC}}$ (36 coupling constants) and $^2J_{\text{HC}}$ (23 coupling constants)) The dotted line represents a 1:1 correspondence.

correspondence between the ^{13}C direct measurement and the calculated data. The average deviation was 0.2 Hz with a maximum of 0.7 for the H3–C5 coupling constant. But for the $^2J_{\text{HC}}$ calculated data showed less correlation compared to the measured $^2J_{\text{HC}}$ coupling constant, with an average deviation of 0.52 Hz and a maximum of 1.18 Hz for the H2–C1 coupling. This larger deviation for the $^2J_{\text{HC}}$ coupling constant could be directly a result of the smaller size of the $^2J_{\text{HC}}$ coupling constant. Most of the DFT calculated coupling constants were smaller than the experimental observed values.

Thus we can see from this subset group of compounds that the $^3J_{\text{HC}}$ for the IPAP-HSQMBC and du8c compare well with the direct measurement of the coupling constants from the ^{13}C NMR with

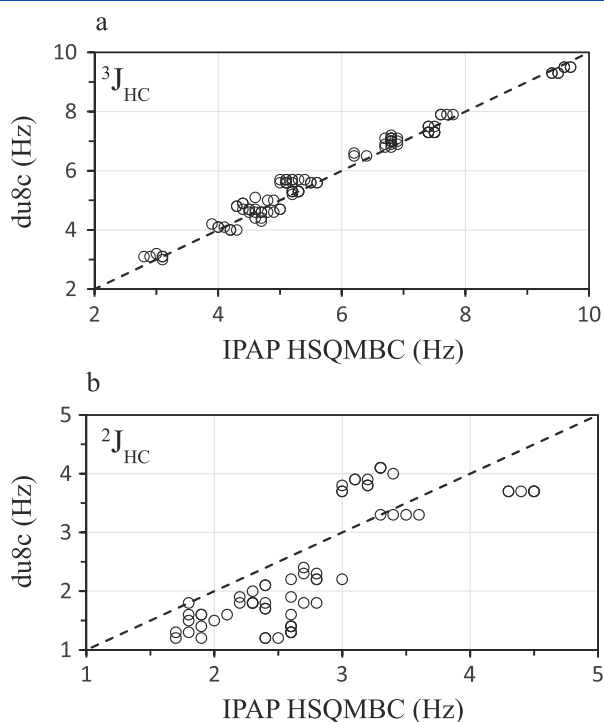


Figure 5. Comparison of the measured and calculated $^3J_{\text{HC}}$ (a) and $^2J_{\text{HC}}$ (b) from the IPAP-HSQMBC NMR and the du8c method ($^3J_{\text{HC}}$ consists of 101 coupling constants) and $^2J_{\text{HC}}$ (consist of 65 coupling constants)). The dotted line represents a 1:1 correspondence.

proton-coupled data. Whereas, the $^2J_{\text{HC}}$ the IPAP-HSQMBC experiment slightly over predicts (probably because of error introduced in the processing of the data and digital resolution) and the du8c under predicts the coupling constants.

Comparing the data for all 12 compounds for the IPAP-HSQMBC experiment with the calculated values from du8c showed a similar result as observed in the subset of the data. The $^3J_{\text{HC}}$ showed that the measured and predicted coupling were in good agreement. Any differences occurred when the du8c predicted slightly large coupling constants. The average deviation was 0.23 Hz with a maximum deviation of 0.7 Hz. Linear regression analysis of this data gave a R^2 of 0.98 resulted with a gradient of 0.96 and a y-intercept of 0.33. For the $^2J_{\text{HC}}$ coupling constants the du8c under predicted almost all of the couplings. Interestingly, the $^2J_{\text{H3C2}}$ couplings were consistently over predicted by 0.6–0.8 Hz in the du8c. Thus, the determination of long-range coupling constants using the above methods has a significant benefit in determining structural details of molecules and provides a deeper understanding of configurational and positional integrity.

Conclusion

The $^nJ_{\text{HC}}$ coupling constants of 12 cinnamic acid based compounds were investigated by experimentally measuring and calculating, by DFT calculations, the $^3J_{\text{HC}}$ and $^2J_{\text{HC}}$ coupling constants. We used a proton-coupled ^{13}C NMR experiment to obtain a 'gold standard' estimates of coupling constants against which we compared other data. A subset of the four compounds was used to compare the experimental and computational methods. The $^3J_{\text{HC}}$ and $^2J_{\text{HC}}$ coupling constants measured by IPAP-HSQMBC compared very well with the couplings derived from the proton-coupled ^{13}C NMR data. The calculated $^3J_{\text{HC}}$ coupling constants

were in good agreement with experimental values, but the $^2J_{\text{HC}}$ coupling constants were predicted to be smaller than the measured values. Comparison of the data from the 12 compounds showed that the $^3J_{\text{HC}}$ coupling constants from the calculated method were slightly higher than the measured values from the IPAP-HSQMBC method, which showed an average deviation of 0.21 Hz. The calculated $^2J_{\text{HC}}$ coupling constants were consistently lower than the measured values from the IPAP-HSQMBC experiment. Our study demonstrates that long-range coupling constants that can be obtained from the proton-coupled ^{13}C NMR spectrum if the multiplet is well resolved and large amounts of the compound are available.

Acknowledgements

This research was funded in part by the Australian Research Council Linkage grant # LP130100703 (DR). This research was supported by the Centre for Advanced Imaging, The University of Queensland and the Queensland NMR network.

References

- [1] W. Koźmiński. *J. Magn. Reson.* **1999**, *137*, 408.
- [2] P. Nolis, T. Parella. *J. Magn. Reson.* **2005**, *176*, 15.
- [3] P. Nolis, J. F. Espinosa, T. Parella. *J. Magn. Reson.* **2006**, *180*, 39.
- [4] K. Kobzar, B. Luy. *J. Magn. Reson.* **2007**, *186*, 131.
- [5] R. A. Edden, J. Keeler. *J. Magn. Reson.* **2004**, *166*, 53.
- [6] R. T. Williamson, B. L. Marquez, W. H. Gerwick, K. E. Kövér. *Magn. Reson. Chem.* **2000**, *38*, 265.
- [7] V. V. Krishnamurthy. *J. Magn. Reson. A* **1996**, *121*, 33.
- [8] W. Koźmiński, D. Nanz. *J. Magn. Reson.* **2000**, *142*, 294.
- [9] A. Meissner, O. W. Sørensen. *Magn. Reson. Chem.* **2001**, *39*, 49.
- [10] S. Gil, J. F. Espinosa, T. Parella. *J. Magn. Reson.* **2011**, *213*, 145.
- [11] J. Saurí, J. F. Espinosa, T. Parella. *Angew. Chem. Int. Ed.* **2012**, *51*, 3919.
- [12] L. Castañar, T. Parella. *Ann. R. NMR S.* **2015**, *84*, 163.
- [13] J. F. Espinosa, P. Vidal, T. Parella, S. Gil. *Magn. Reson. Chem.* **2011**, *49*, 502.
- [14] T. Parella, J. F. Espinosa. *Prog. Nucl. Magn. Reson. Spectrosc.* **2013**, *73*, 17.
- [15] J. Saurí, T. Parella, J. F. Espinosa. *Org. Biomol. Chem.* **2013**, *11*, 4473.
- [16] A. Bagno, G. Saielli. *Theor. Chem. Acc.* **2007**, *117*, 603.
- [17] V. Barone, R. Improta, N. Rega. *Acc. Chem. Res.* **2008**, *41*, 605.
- [18] G. Bifulco, P. Dambruoso, L. Gomez-Paloma, R. Riccio. *Chem. Rev.* **2007**, *107*, 3744.
- [19] L. B. Casabianca, A. C. de Dios. *J. Chem. Phys.* **2008**, *128*, 052201.
- [20] T. Helgaker, M. Jaszunski, K. Ruud. *Chem. Rev.* **1999**, *99*, 293.
- [21] M. W. Lodewyk, M. R. Siebert, D. J. Tantillo. *Chem. Rev.* **2011**, *111*, 1117.
- [22] F. A. A. Mulder, M. Filatov. *Chem. Soc. Rev.* **2010**, *39*, 578.
- [23] A. G. Petrovic, A. Navarro-Vazquez, J. L. Alonso-Gomez. *Curr. Org. Chem.* **2010**, *14*, 1612.
- [24] H. U. Siehl. *Adv. Phys. Org. Chem.* **2007**, *42*, 125.
- [25] P. H. Willoughby, M. J. Jansma, T. R. Hoye. *Nat. Protoc.* **2014**, *9*, 643.
- [26] A. G. Kutateladze, O. A. Mukhina. *J. Org. Chem.* **2015**, *80*, 5218.
- [27] V. Bankova. *J. Nat. Prod.* **1990**, *53*, 821.
- [28] G. V. Ambulgekar, B. M. Bhanage, S. D. Samant. *Tetrahedron Lett.* **2005**, *46*, 2483.
- [29] Z. Zhang, Z. Zha, C. Gan, C. Pan, Y. Zhou, Z. Wang, M.-M. Zhou. *J. Org. Chem.* **2006**, *71*, 4339.
- [30] Z. Zhang, Z. Wang. *J. Org. Chem.* **2006**, *71*, 7485.
- [31] A. Ianni, S. R. Waldvogel. *Synthesis* **2006**, 2103.
- [32] J. C. Facelli. *J. Phys. Chem. B* **1998**, *102*, 2111.
- [33] G. Saielli, K. Nicolaou, A. Ortiz, H. Zhang, A. Bagno. *J. Am. Chem. Soc.* **2011**, *133*, 6072.
- [34] A. G. Kutateladze, O. A. Mukhina. *J. Org. Chem.* **2015**, *80*, 10838.
- [35] D. Doddrell, D. Pegg, M. R. Bendall. *J. Magn. Reson.* **1982**, *48*, 323.

Supporting information

Additional supporting information may be found in the online version of this article at the publisher's web site.